

Iron nanoparticle bio-interactions evaluated in *Xenopus laevis* embryos, a model for studying the safety of ingested nanoparticles

Patrizia Bonfanti, Anita Colombo, Melissa Saibene, Luisa Fiandra, Ilaria Armenia, Federica Gamberoni, Rosalba Gornati, Giovanni Bernardini & Paride Mantecca

To cite this article: Patrizia Bonfanti, Anita Colombo, Melissa Saibene, Luisa Fiandra, Ilaria Armenia, Federica Gamberoni, Rosalba Gornati, Giovanni Bernardini & Paride Mantecca (2019): Iron nanoparticle bio-interactions evaluated in *Xenopus laevis* embryos, a model for studying the safety of ingested nanoparticles, *Nanotoxicology*, DOI: [10.1080/17435390.2019.1685695](https://doi.org/10.1080/17435390.2019.1685695)

To link to this article: <https://doi.org/10.1080/17435390.2019.1685695>



© 2019 The Author(s). Published by Informa UK Limited, trading as Taylor & Francis Group



[View supplementary material](#)



Published online: 13 Nov 2019.



[Submit your article to this journal](#)



[View related articles](#)



[View Crossmark data](#)

Iron nanoparticle bio-interactions evaluated in *Xenopus laevis* embryos, a model for studying the safety of ingested nanoparticles

Patrizia Bonfanti^a, Anita Colombo^a, Melissa Saibene^a, Luisa Fiandra^a, Ilaria Armenia^b, Federica Gamberoni^b, Rosalba Gornati^b, Giovanni Bernardini^b and Paride Mantecca^a

^aDepartment of Earth and Environmental Sciences, Research Centre POLARIS, University of Milano-Bicocca, Milano, Italy; ^bDepartment of Biotechnology and Life Sciences, University of Insubria, Varese, Italy

ABSTRACT

Iron nanoparticles (NPs) have been proposed as a tool in very different fields such as environmental remediation and biomedical applications, including food fortification against iron deficiency, even if there is still concern about their safety. Here, we propose *Xenopus laevis* embryos as a suitable model to investigate the toxicity and the bio-interactions at the intestinal barrier of Fe₃O₄ and zerovalent iron (ZVI) NPs compared to Fe(II) and (III) salts in the 5 to 100 mg Fe/L concentration range using the Frog Embryo Teratogenesis Assay in *Xenopus* (FETAX). Our results demonstrated that, at concentrations at which iron salts induce adverse effects, both iron NPs do not cause acute toxicity or teratogenicity even if they accumulate massively in the embryo gut. Prussian blue staining, confocal and electron microscopy allowed mapping of iron NPs in enterocytes, along the paracellular spaces and at the level of the basement membrane of a well-preserved intestinal epithelium. Furthermore, the high bioaccumulation factor and the increase in embryo length after exposure to iron NPs suggest greater iron intake, an essential element for organisms. Together, these results improve the knowledge on the safety of orally ingested iron NPs and their interaction with the intestinal barrier, useful for defining the potential risks associated with their use in food/feed fortification.

ARTICLE HISTORY

Received 26 July 2019
Revised 27 September 2019
Accepted 22 October 2019

KEYWORDS



Food supplementation; iron nanoparticles; *Xenopus laevis*; developmental toxicity; FETAX


Introduction

Iron-based nanoparticles (NPs) are currently used in very different fields ranging from environmental remediation to nanomedicine. In particular, zero-valent (ZVI) iron NPs have gained increasing attention for soil, groundwater and wastewater remediation. Indeed, thanks to their reduced size, ZVI NPs applied *in situ* show higher reactivity towards a wide range of aqueous contaminants (inorganic anions, chlorinated organic compounds and heavy metals) and higher mobility compared to their microscale counterpart (Li et al. 2017). Nevertheless, these advantages are undermined when the mobility potential away from the injection site is limited both by NP-specific physical-chemical properties and environmental/hydrogeological conditions (pH, dissolved oxygen and oxidation-reduction potential, dissolved organic matter)

that determine the aggregation/agglomeration of NPs and their consequent sedimentation (Grieger et al. 2010). These phenomena can lead to the formation of ZVI hotspots that represent a source of contamination for benthic organisms, which are in turn relevant for the transfer of ZVI NPs to other organisms through the food chain, in particular to those that graze on the bottom such as fish and amphibian larvae.

Among nanoscale iron, superparamagnetic iron oxide NPs are widely studied for magnetic resonance imaging (MRI), for cancer treatment (Song et al. 2019) and for targeting antibiotics (Armenia et al. 2018), enzymes (Balzaretto et al. 2017) and other drugs (Moros et al. 2018). In addition, iron NPs functionalized with thermophilic enzymes might find their place also in industrial biotechnology (Armenia et al. 2019).

CONTACT Anita Colombo  anita.colombo@unimib.it  Department of Earth and Environmental Sciences, Research Center POLARIS, University of Milano Bicocca, 1, Piazza della Scienza, 20126 Milano, Italy.

 Supplemental data for this article can be accessed [here](#).

© 2019 The Author(s). Published by Informa UK Limited, trading as Taylor & Francis Group

This is an Open Access article distributed under the terms of the Creative Commons Attribution-NonCommercial-NoDerivatives License (<http://creativecommons.org/licenses/by-nc-nd/4.0/>), which permits non-commercial re-use, distribution, and reproduction in any medium, provided the original work is properly cited, and is not altered, transformed, or built upon in any way.

Recently, the use of iron NPs in nanomedicine is also arousing interest in food and feed iron supplementation. Indeed, iron deficiency is common in several physiological and pathological conditions (Camaschella 2019), and is particularly evident in developing countries (Kassebaum et al. 2016). The water-soluble and bioavailable ferrous sulfate, fumarate or gluconate, currently used for controlling iron deficiency, unfortunately, affect the gastrointestinal tract with significant side effects (Tolkien et al. 2015). Conversely, the good bioavailability, product stability, negligible side effects and no changes of food organoleptic properties of iron NPs make them eligible for food fortification (Rohner et al. 2007; Hilty et al. 2010; Zimmermann et al. 2011; Hosny et al. 2015).

Considering the various applications described above, iron-based NPs raise concerns for the potential risk of exposure through ingestion, which can occur both into the aquatic environment, this being the ultimate recipient of NPs that are intentionally or accidentally spilled into it, and when they are used as nanoingredients. *In vitro* (Gornati et al. 2016; Coccini et al. 2019) and *in vivo* experiments on mammals (Cappellini et al. 2015; Feng et al. 2018) have been performed to evaluate iron NP toxicity. Moreover, several iron NPs (i.e. FePO₄ NPs) have proven to be safe for ingestion in parallel studies on rat and human cell lines (von Moos et al. 2017). Nevertheless, limited studies are available that relate NP effects to the modality of nano-bio interactions on alternative models, especially during the sensitive period of early development (Valdiglesias et al. 2015).

Embryos of *Xenopus laevis* have been used for a long time in toxicology and proved so well their suitability that, in 1983, Dumont and colleagues (Dumont et al. 1983) conceived a test, the Frog Embryo Teratogenesis Assay in *Xenopus* (FETAX) that was making use of *Xenopus* embryos. This bioassay, thanks to its three end-points (i.e. mortality, malformation and growth retardation), was mainly designed for the evaluation of developmental toxicants, predicting human teratogens with a 75% accuracy (Fort and Robbin 2002). FETAX has been used not only for evaluating single compounds (Bernardini et al. 1994; Presutti et al. 1994), but also to test environmental mixtures (Dawson 1991; Fort et al. 2003), soils (Prati et al. 2000), sludges (Chenon et al. 2003), the efficiency of an environmental plan (Vismara et al. 1993) or to study the decline of

amphibian population (Garber et al. 2004). Recently, FETAX has become useful also for evaluating toxicity and teratogenicity of nanomaterials (Bacchetta et al. 2012; Colombo et al. 2017).

The utility of the FETAX can further be enhanced adding to the whole embryo morphological end-points, sub-organismal and molecular studies with the aim of obtaining mechanistic information (Fort, McLaughlin, and Burkhart 2003). As we have shown in previous papers, *Xenopus laevis* embryos can provide insights for evaluating NP bio-interactions in particular at the intestinal barrier (Bacchetta et al. 2012; Bonfanti et al., 2015; Colombo et al. 2017). In fact, contrary to other non-mammalian embryos (e.g. zebrafish and medaka), typically used for ecotoxicological and developmental studies, *Xenopus* embryos during the first 96 h of development complete the organogenesis and with the stomodeum opening (stage 40, 2 day and 18 h p.f. at 23 °C) begin to ingest materials present in the environment. Therefore, the ingested materials come into contact very early with an epithelial monolayer of enterocytes with microvilli that increase the cell surface area facing gut lumen quite similar to that of the mammalian gut.

In this paper, we propose *X. laevis* embryos as a model for studying iron NP bio-interactions and evaluate their safety. Here, we have shown that embryos accumulate NPs in the intestine. The massive presence of iron NPs in the embryo intestine, however, does not seem to cause acute toxicity nor teratogenicity. This model is also promising for studying NP diffusion across the intestine. Indeed, paracellular pathway, endocytosis-exocytosis, M-cell-mediated pathway (Yu et al. 2016) as well as simple diffusion by direct crossing of the plasma membrane (Zanella et al. 2017) are the mechanisms by which NPs are supposed to cross the intestinal biological barrier.

Material and methods

Chemicals and iron NPs

Zerovalent iron (ZVI) NPs were purchased from American Elements (Los Angeles, CA, USA). They were supplied in form of nanopowder, with 99% purity and aerodynamic particle size <100 nm, composed by NPs with a primary size of 20–40 nm as described by the supplier. Iron oxide (Fe₃O₄) NPs (CAS Number 1317-61-9) were purchased in form of nanopowder with a

TEM determined size <50 nm as declared by the supplier (Sigma-Aldrich, St. Louis, USA).

Stock suspensions of both iron NPs were prepared in deionized (DI) water at a concentration of 10 g Fe/L and sonicated for 15 min. Working concentrations of NPs (5, 10, 50 and 100 mg Fe/L) were obtained by diluting stock solutions in FETAX solution. FETAX solution composition was (in mg/L): 625 NaCl, 96 NaHCO₃, 30 KCl, 15 CaCl₂, 60 CaSO₄·2H₂O and 70 MgSO₄ (pH 7.6–8.0). Suspensions were vortexed for 30 sec to obtain homogeneous dispersions.

All analytical-grade reagents, human chorionic gonadotropin (HCG), 3-amino-benzoic acid ethyl ester (MS222), salts for FETAX solution, iron(III) chloride (FeCl₃) and iron(II) sulfate heptahydrate (FeSO₄·7H₂O) were purchased from Sigma-Aldrich S.r.l., Italy.

NP characterization

The primary size and shape of ZVI and Fe₃O₄ NPs were evaluated with a JEOL-1010 electron microscope (JEOL, Tokyo, Japan) operating at 90 kV and equipped with a CCD camera MORADA (Olympus, Tokyo, Japan). Samples were prepared placing 5 μl of a diluted suspension of each NP type in ethanol on a formvar-carbon-coated copper grid.

Hydrodynamic diameter (D_h) and ζ-potential of iron NPs were evaluated in deionized water at a concentration of 25 mg Fe/L with a Zetasizer Nano ZS90 (Malvern Instruments, UK). The D_h was measured in a clear 2 mL cuvette and the ζ-potential in 1 mL folded capillary cell (DTS1061, Malvern Instruments, UK) at room temperature, immediately after vortexing the sample.

Monitoring of iron NP behavior in FETAX solution

Stocks of freshly prepared ZVI and Fe₃O₄ NPs were diluted in FETAX solution at nominal concentrations of 25 and 100 mg Fe/L. Temporal changes of pH of NP suspensions and iron salt solutions were monitored *ex situ* for 24 h at room temperature. NP sedimentation was monitored for 24 h at room temperature in clear 2 mL polypropylene cuvettes with a UV-vis spectrophotometer at 506 nm.

Since during FETAX test the treatment solutions were renewed every 24 h, NP dissolution in FETAX solution was quantified at 24 h, by collecting the iron NP suspensions from three test replicates

directly from the Petri dishes before renewal. To remove the non-soluble fraction of NPs, samples were ultra-filtrated with ultra-filtration centrifuge tubes with a 10 kDa molecular weight cutoff (Vivaspin®6, 10000 MWCO PES, Sartorius, Germany) at 4000 g for 15 min at room temperature. Filtrates were acidified by adding HNO₃ to a final concentration of 2% and measured with an ICP-OES (Perkin-Elmer Optima 7000 DV, Santa Clara, CA, USA). The analyses were conducted on samples from three independent bioassays and each measurement was replicated three times.

Experimental design

The embryotoxicity was assessed using the conventional FETAX protocol in which *Xenopus* embryos at mid-blastula stage (5 h post fertilization, p.f.) (Nieuwkoop and Faber 1956) were exposed to freshly prepared iron NP suspensions and to FeSO₄ and FeCl₃ solutions. The concentration range (5–100 mg Fe/L) was selected in order to obtain a good concentration response curve, in terms of mortality and malformations, and therefore, allow calculation of the LC₅₀ and EC₅₀ of the most active compounds. Control embryos were incubated in standard FETAX solution alone. At the end of the tests, 96 h p.f. embryos were processed for histopathology, ferric and ferrous ions localization, NP tracking by confocal and electron microscopy and iron accumulation by ICP-OES.

Fetax

Xenopus laevis embryos were generated and tests were conducted as previously described (Bonfanti et al. 2015). Briefly, before embryo selection, the jelly coat was removed by swirling the embryos for 1 to 2 min in a 2.25% L-cysteine solution (pH 8.1). Each single test consisted of three replicates for control and two technical replicates for each compound concentration. For each compound at least three tests were performed. All of the Petri dishes were incubated in a thermostatic chamber at 23 ± 0.5 °C with a mild shaking until the end of the test (96 h p.f.). All treatment solutions and NP suspensions were freshly prepared and renewed daily after the counting and removal of dead embryos.

At the end of the test, the surviving embryos of each experimental group were anesthetized with MS-222 (100 mg/L) and screened for individual morphological abnormalities with a stereo-microscope (Zeiss, Germany), taking as a reference the Atlas of Hausen and Riebesell (1991). The embryos were then formalin fixed to estimate the growth retardation by measuring head-tail length with the digitizing software AxioVision.

Histopathological analysis

For light microscopy analyses, embryos were randomly selected at the end of the FETAX assays, fixed in 10% buffered formalin and processed for embedding in paraffin. The samples were transversely cut from eye to proctodeum into 6 μm thick serial sections, and mounted on glass slides. Sections were alternatively stained with hematoxylin and eosin (H&E) for histopathological analysis and Prussian blue or Turnbull staining for evidencing tissue Fe(III) or Fe(II) deposits. Sections were finally examined with a Zeiss Axioplan light microscope, equipped with an Axiocam MRc5 digital camera. Ten specimens for each experimental group were histologically screened.

Iron NP tracking by confocal reflection microscopy

For NP visualization in the embryo intestinal epithelium, a Leica TCS SP5 confocal laser scanning microscope (CLSM) was used in reflection mode. Embryos were fixed overnight in 10% buffered formalin at room temperature, rinsed and bleached in a $\text{H}_2\text{O}_2/\text{KOH}$ (3%/0.5%) solution for 2 h to avoid reflection due to embryo pigmentation (Bacchetta et al. 2014). After processing with standard histological procedures, the sections, mounted on glass slides, were dewaxed, hydrated and processed for rhodamine phalloidin staining to visualize brush border actin filaments (Colombo et al. 2017). According to Prins and colleagues (Prins, Velde, and de Heer 2006), samples were illuminated with a 488-nm argon/krypton laser using an intensity of the AOTF filter of 10%. A neutral RT 30/70 filter was used as beam splitter and placed at a 45 angle in the path of the beam. Images were processed with the Leica dedicated LAS AF software.

Electron microscopy analysis

For TEM analyses, embryos were randomly selected at the end of the FETAX assays and fixed in 2.0% paraformaldehyde and 0.2% glutaraldehyde in 0.1 M phosphate buffer at pH 7.4. After several washes in the same buffer, embryos were post-fixed in 1% OsO_4 in 0.1 M phosphate buffer at pH 6.0 for 1.5 h at 4 °C in the dark, washed with milliQ water, counterstained with 1% uranyl acetate, dehydrated in a graded ethanol series, and transferred in 100% propylene oxide. Infiltration was performed with propylene oxide and embedding resin (Araldite-Epon) at volumetric proportions of 2:1 for 1.5 h, 1:1 overnight, 1:2 for 1.5 h and pure resin for 4 h. Samples were polymerized at 60 °C for 48 h. Ultra-thin sections were cut with a Reichert Ultracut E microtome and collected on 200-mesh uncoated copper grids. Sections were not counterstained to avoid contaminations by lead citrate and uranyl acetate that ultimately may interfere with metal NP visualization. Samples were analyzed using a Jeol JEM1220 transmission electron microscope operating at an accelerating voltage of 80 kV and equipped with a Lheritier LH72WA-TEM digital camera.

Iron quantification in embryos

At the end of the test, control and treated embryos were collected and placed in Petri dishes containing fresh FETAX solution for 36 h to purge them from ingested NPs still present in the intestinal lumen or attached to the embryo surface. Embryos (approximately 100 embryos per measurement) were then weighted and quickly frozen on dry ice and stored at -80 °C until analyses.

For Fe bioaccumulation determination, embryos were dried until complete water loss occurred (about 3 h at 50 °C). Embryos were then digested in 4 ml of 65% iron-free HNO_3 using a mineralizator Milestone Ethos TC (Milestone srl, Italy). After adequate dilution, samples were analyzed by ICP-OES (PerkinElmer, Optima 7000 DV Perkin Elmer) to quantify total iron concentrations. Each measurement was repeated three times.

Data collection and statistical analysis

The number of dead embryos *versus* their total number at the beginning of the test led to the mortality percentages, and the number of malformed

embryos *versus* the total number of surviving ones gave the malformed embryo percentages. Data were expressed as the mean \pm SEM. The data were tested for homogeneity and normality.

When these assumptions were met, one-way analysis of variance (ANOVA) was performed; otherwise, the non-parametric Kruskal–Wallis test was applied. The significance level was set at $p < 0.05$. The incidence of specific malformations was investigated by chi-square method, using Yates's correction for continuity (χ^2 test) or Fisher's exact tests. Mortality and malformation percentages were used to calculate the 96 h p.f. LC₅₀ (concentration causing 50% lethality) and 96 h p.f. EC₅₀ (concentration inducing teratogenesis in 50% of surviving embryos) for each experimental group. These values were calculated resorting to Probit analysis (Bernardini et al. 1994) and to this aim the IBM SPSS statistic 25 software has been used with 95% confidence interval. The Teratogenic Index (TI), useful in estimating the teratogenic risk associated with the tested compounds, is represented by the LC₅₀/EC₅₀ ratio.

Results

Characterization of iron NPs

TEM micrographs confirm the NP size and shape declared by the suppliers for both types of iron NPs, although the size and shape variability seemed to be larger (Figure 1). Fe₃O₄ NPs show round shapes, while ZVI NPs have a more polygonal surface area.

DLS analysis on NPs suspension in distilled water and FETAX solution showed a dispersion of larger NPs that rapidly agglomerate, yielding a high polydispersity index (PDI) (Table S1 in Supplementary Material). The ζ potential measurements of iron NPs, performed at a concentration of 25 mg/L in distilled water and recorded at 25 °C, resulted to be -12.5 mV for ZVI NPs and $+9.4$ for Fe₃O₄ NPs. Moreover, these values suggest a tendency of NPs to agglomerate.

Behavior of iron NPs in FETAX solution

The pH values of iron salt solutions (FeSO₄ and FeCl₃) (Figure S1 in Supplementary Material) and NP suspensions at the concentrations of 25 and 100 mg Fe/L were measured over 24 h. It is known that Fe(III) solutions undergo acid hydrolysis and that during aging also Fe(II) ions and Fe⁰ in aqueous solution at alkaline pH, such as that of FETAX solution, oxidize to Fe(III). In our hands, 25 mg Fe/L of FeSO₄ and FeCl₃ salts caused a decrease of FETAX solution pH from pH 7.7 to 6.2 and 6.9, respectively. These values, however, are still compatible with embryo development (Bonfanti et al. 2018). Instead, 100 mg Fe/L of FeSO₄ and FeCl₃ produced, within 24 h, a drastic decrease of the pH of the FETAX solution to 5.2 and to 4, respectively. On the contrary, equivalent concentrations of iron NPs did not reduce the pH of FETAX solution to values lower than 6.8, in agreement with their low dissolution (reported in Figure 2).

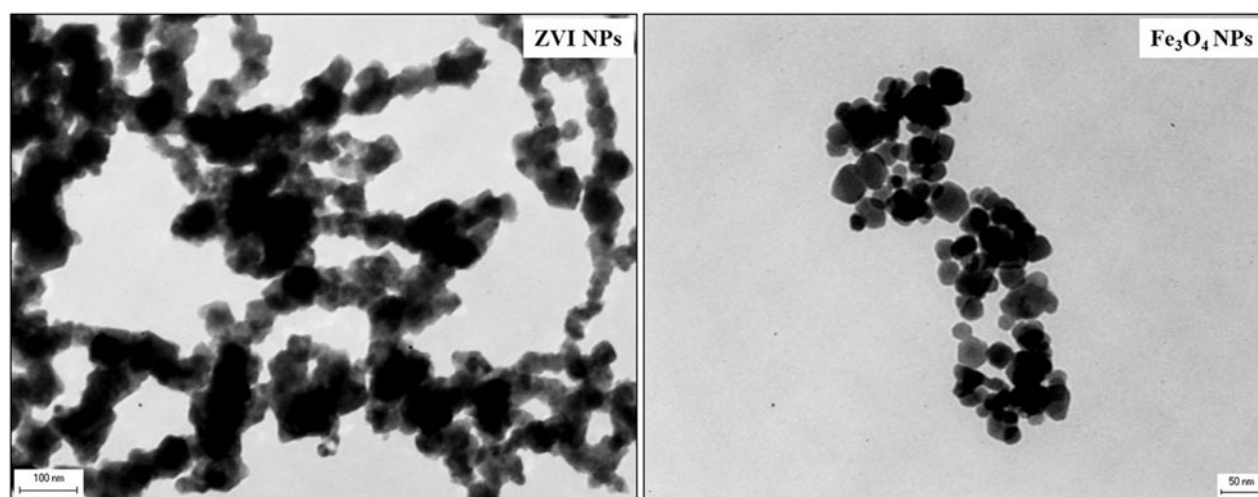


Figure 1. Transmission electron microscopy of iron NPs. The analysis revealed the large heterogeneity in the NP size and shape. Scale bar: ZVI NPs 100 nm; Fe₃O₄ NPs 50 nm.

The settling properties analysis of ZVI and Fe₃O₄ NPs in FETAX solution showed that large agglomerates of both NPs tended to precipitate as a function of time and concentration as shown in Figure S2 in Supplementary Material. After 24 h, however, only a small percentage of NPs remained in suspension (approximately 6% for the 25 mg Fe/L suspensions and 3% for the 100 mg Fe/L suspensions).

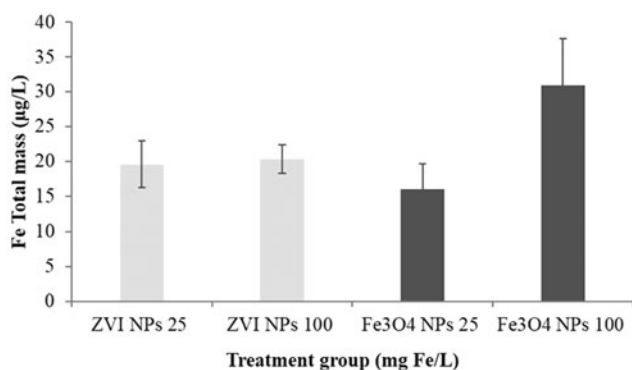


Figure 2. Dissolution of iron NPs in FETAX medium. Measures were performed at 25 and 100 mg Fe/L NPs at 24 h by ICP-OES after removal of NPs by ultrafiltration. Histograms represent the mean concentrations of soluble Fe in NP suspensions ($n = 3$). Bars = standard error of the mean (SEM).

To evaluate the contribution of dissolved ions to NP embryotoxicity, the dissolution of ZVI and Fe₃O₄ NPs in the FETAX solution was tested by ICP-OES after 24 h (Figure 2). The soluble iron concentrations measured in the NP-free ultrafiltrates of both suspensions ranged from 16 to 31 µg/L. These results demonstrate that ZVI and Fe₃O₄ NPs are poorly soluble in the saline solution used for the biological tests. If the data are expressed as a percentage of dissolved iron with respect to the total nominal mass, the dissolved iron was 0.08 and 0.06% for 25 mg Fe/L ZVI and Fe₃O₄ NPs, and 0.02 and 0.03% for 100 mg Fe/L ZVI and Fe₃O₄ NPs, respectively. Therefore, the increased particle agglomeration and precipitation observed with NP suspension at a concentration of 100 mg Fe/L might prevent extensive dissolution.

Comparative embryotoxicity of iron NPs and salts

Figure 3(A) shows the concentration-response curves for mortality and malformed embryos after exposure to ZVI and Fe₃O₄ NPs and iron salt solutions. Iron NPs were not embryo-lethal even at the highest tested concentration (100 mg Fe/L), as mortality rates were

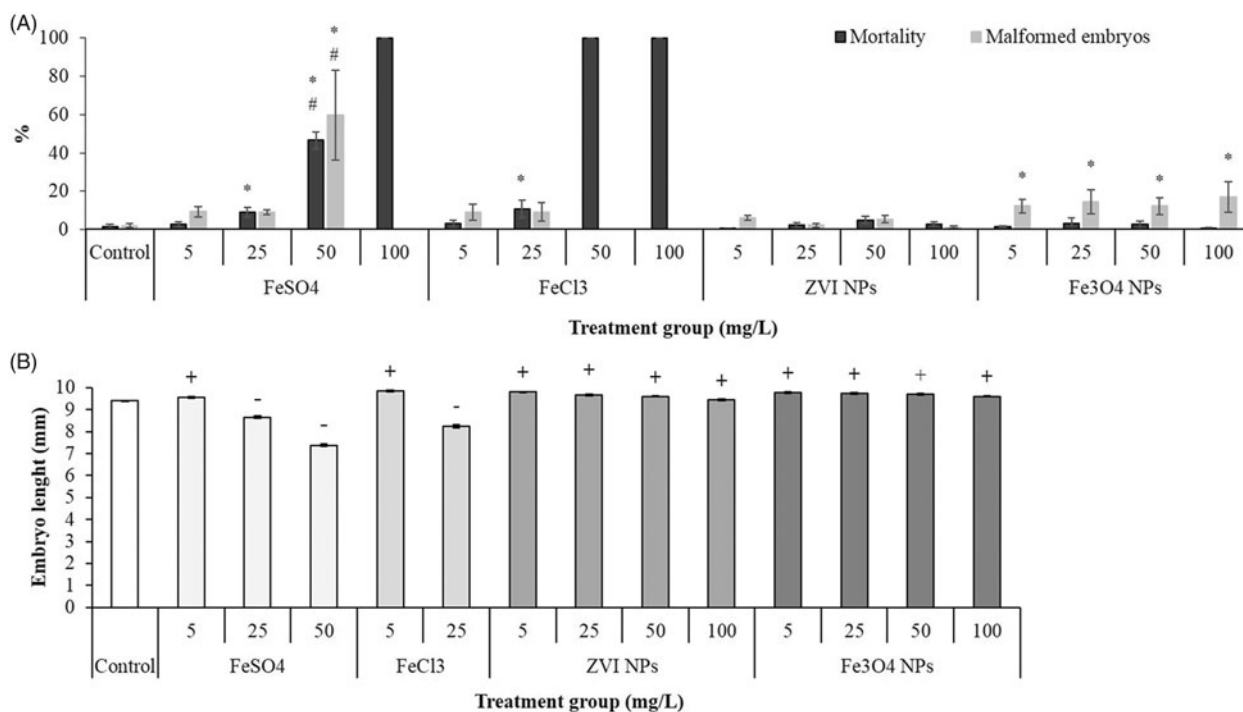


Figure 3. FETAX results after exposure to iron NPs and Fe (II/III) salts. (A) Comparative embryotoxicity expressed as mortality and malformed embryo rates. (B) Effect on growth expressed as head-tail length of stage 46 *X. laevis* embryos. All values are given as mean \pm SEM of three independent assays. In (A): (*) statistically different from control; (#) statistically different from the corresponding concentration of iron salt or NPs ($p < 0.05$, ANOVA + Fisher LSD Method). In (B): (+) statistically significant increase versus control; (-) statistically significant decrease versus control ($p < 0.05$, ANOVA + Dunn's test).

Table 1. Pattern of malformations in stage 46 *Xenopus* embryos exposed to iron NPs and Fe(II)/(III) salts.

	FeSO ₄ (mg Fe/L)				FeCl ₃ (mg Fe/L)		ZVI NPs (mg Fe/L)				Fe ₃ O ₄ NPs (mg Fe/L)			
	Control	5	25	50	5	25	5	25	50	100	5	25	50	100
Total embryos	428	121	125	125	201	198	225	225	225	225	200	200	200	202
Living embryos	428	118	113	68	195	177	224	219	214	218	197	194	195	201
Gut miscoiling	7 (1.6)	9 (7.6) ^b	9 (8.0) ^b	35 (51.5) ^b	14 (7.2) ^b	4 (2.3)	8 (3.6)	3 (1.4)	8 (3.7)	1 (0.5)	13 (6.6) ^b	16 (8.2) ^b	15 (7.7) ^b	19 (9.5) ^b
Abdominal edema				3 (4.4) ^b			1 (0.4)	1 (0.5)	1 (0.5)		5 (2.5) ^b	8 (4.1) ^b	6 (3.1) ^b	11 (5.5) ^b
Tail flexure			1 (0.9)	8 (11.8) ^b	2 (1.0) ^a		1 (0.4)		2 (0.9)		2 (1.0) ^a		2 (1.0) ^a	3 (1.5) ^a
Craniofacial defects		1 (0.8)	1 (0.9)	6 (8.8) ^b	2 (1.0) ^a			1 (0.5)			2 (1.0) ^a			
Eye defects	2 (0.46)		1 (0.9)	2 (2.9) ^a	3 (1.5)		1 (0.4)	1 (0.5)			1 (0.5)		1 (0.5)	

(Percentages based on number of malformations/number of those living)

^aChi-squared test: $p < 0.001$ versus control.

^bChi-squared test: $p < 0.05$ versus control.

not statistically different from control and never exceeded 5%. In contrast, both Fe(II) and Fe(III) salts caused a mortality rate statistically different from controls, already at the concentration of 25 mg Fe/L. FeCl₃, however, produced a stronger acute toxic effect since at 50 mg Fe/L and within 24 h caused the death of all the embryos. Significant amounts of Fe(III) hydroxide precipitates were adsorbed on the surface of fertilization envelope at 24 h p.f. (data not shown).

Malformation rates statistically different from controls occurred to embryos exposed to iron salts and iron oxide NPs. Morphological analysis evidenced abnormalities of the tail, face, eyes, and gut coiling often associated with the presence of edema in the abdominal region (Table 1 and Figure 4).

However, such malformations occurred in the same concentration range at which mortality occurred. Therefore, the tested compounds are not to be considered teratogens as established by the Teratogenic Index (TI) calculated as the ratio between 96 h pf LC₅₀ and EC₅₀ reported in Table 2.

As far as it concerns the third FETAX endpoint, i.e. growth inhibition, the head-tail length of living embryos has been measured. The data showed a significant growth inhibition after exposure to both Fe(II) and Fe(III) salts at already 25 mg Fe/L (Figure 3(B)). Interestingly, the lowest concentration of iron salts (5 mg Fe/L) and all the tested concentrations of iron NPs caused an increment of the embryo lengths respect to those of the control group (Figure 3(B)). This deviation from the commonly described monotonic behavior of the concentration-response curves, suggests a hormetic effect (Prati et al. 2002).

Histopathological analysis and NP tracking

The observation of serial transverse histological sections of 96 h old embryos exposed to 25 mg Fe/L

confirmed that primary organogenesis was not substantially impaired by treatments with iron salts and NPs (Figure 5(A–E)). Focusing on gut epithelium at higher magnification, some morphological alterations such as a slightly damaged brush border and sporadic aggregations of yolk platelets in enterocytes were detected in embryos treated with both iron salts and NPs (Figure 5(G–L)). These data suggest a delay in the differentiation of the intestinal epithelium that is more evident in embryos treated with iron salts than in those treated with iron NPs (Figure 5(G–H)).

Furthermore, the presence of debris in the intestinal lumen was evident, especially in the intestine of embryos treated with iron NPs. Perl's staining confirmed that iron in form of Fe(III) accumulated in the gastrointestinal tract of treated groups (Figure 6). In addition to the large iron clusters present in the intestinal lumen, the blue staining showed that iron adheres to the brush border (Figure 6(H–L)). The blue staining is present also in the cytoplasm of the enterocytes in particular in Fe₃O₄ NP treated embryos (Figure 6(L)). Turnbull staining did not reveal the presence of ferrous iron (data not shown).

The tracking of iron NPs performed by the confocal microscope in reflection mode showed the interaction of iron NPs with the intestinal epithelium (Figure 7). In particular, iron NPs were mapped along the microvilli, at the level of intestinal epithelium basement membrane, and dispersed within the enterocytes. In embryos treated with ZVI, NPs were also observed in the paracellular spaces (Figure 7(B)). Instead, Fe₃O₄ NPs were observed even at the level of the serous membrane lining the abdominal cavity (Figure 7(C)).

To better detail the iron NP interaction with the intestinal epithelium, we carried out an

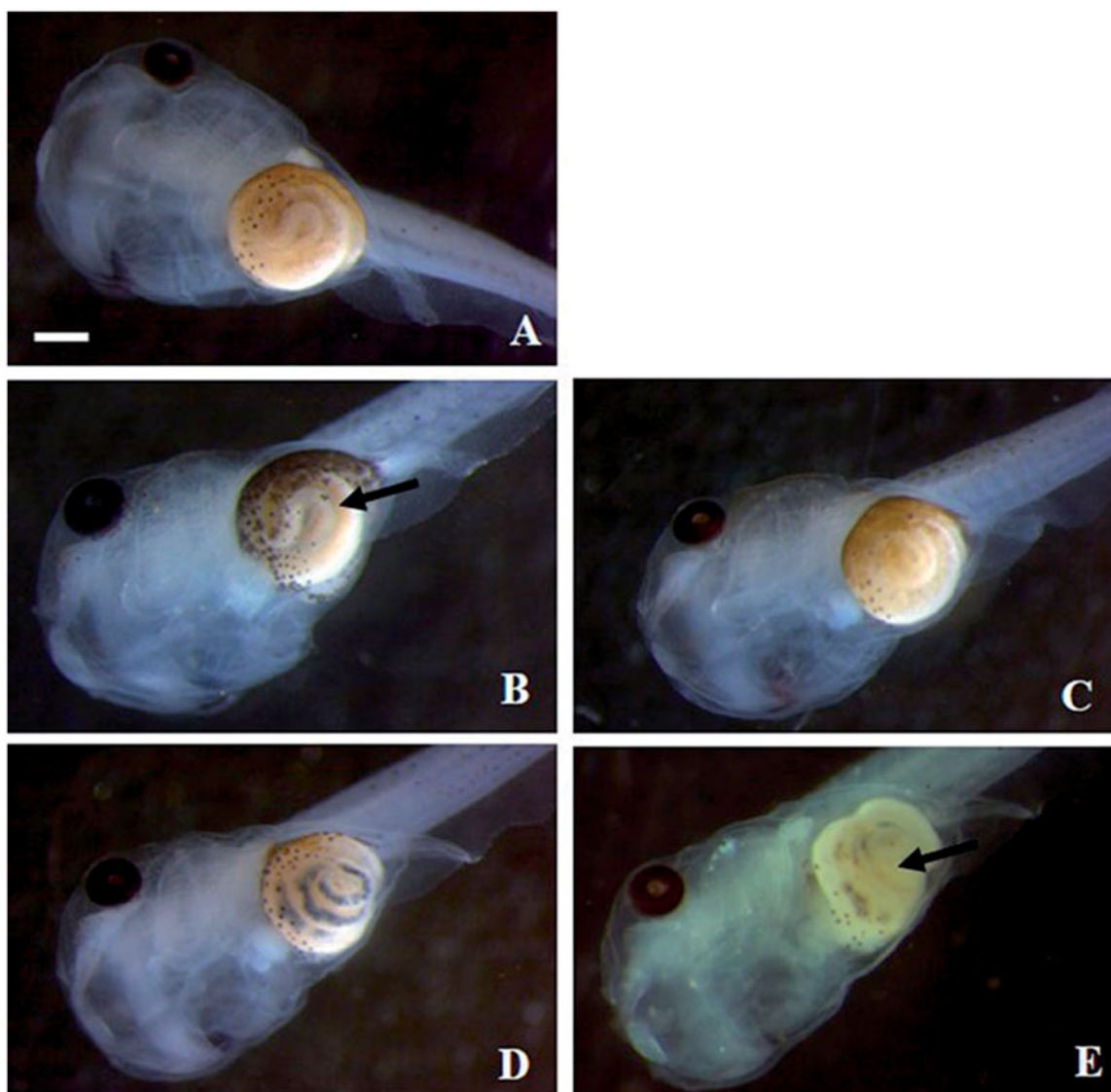


Figure 4. *Xenopus laevis* embryos at the end of the FETAX test. Ventral views of a control (A) and embryos exposed to 25 mg Fe/L of FeSO_4 (B), FeCl_3 (C), ZVI NPs (D) and Fe_3O_4 NPs (E). FeSO_4 treated embryos show abnormal gut coiling (arrow) and the presence of dark material in the intestinal loops is appreciable in NP treated embryos (D and E). Bars = 500 μm .

Table 2. Embryotoxicity of Fe(II) and (III) salts and iron NPs in 96 h pf *Xenopus laevis* embryos.

96 hpf			
Treatment	LC ₅₀ (mg/L)	EC ₅₀ (mg/L)	TI
FeSO_4	56.10 (41.80-81.86)	79.14 (n.d.)	0.7
FeCl_3	32.21 (14.53-87.48)	74.14 (n.d.)	0.43
ZVI NPs	n.d.	n.d.	n.d.
Fe_3O_4 NPs	n.d.	232.68 (n.d.)	n.d.

n.d.: not determined; LC₅₀: Median lethal concentration; EC₅₀: Median teratogenic concentration; TI: Teratogenic index (LC₅₀/EC₅₀).

ultrastructural analysis by TEM, which confirmed the presence of NP aggregates associated with microvilli (Figure 8(C,F)) and cytoplasmic yolk platelets (Figure 8(D,G,E)), and their translocation up to enterocyte basal region (Figure 8(H)).

Moreover, the Fe_3O_4 NP aggregates were also found in proximity of hepatic sinusoidal spaces and within hepatocytes, demonstrating that at least these iron NPs were transferred from the enterocytes to blood circulation and internalized by hepatocytes (Figure 9). However, although we did not find ZVI NPs near the hepatocytes in the observed samples, we cannot exclude their transfer to the bloodstream.

Bioaccumulation in embryos

Bioaccumulation of iron in embryo tissues after exposure to iron salts and NPs at the nominal concentration of 25 mg Fe/L is reported in Figure 10. A significant increase in iron body intake was

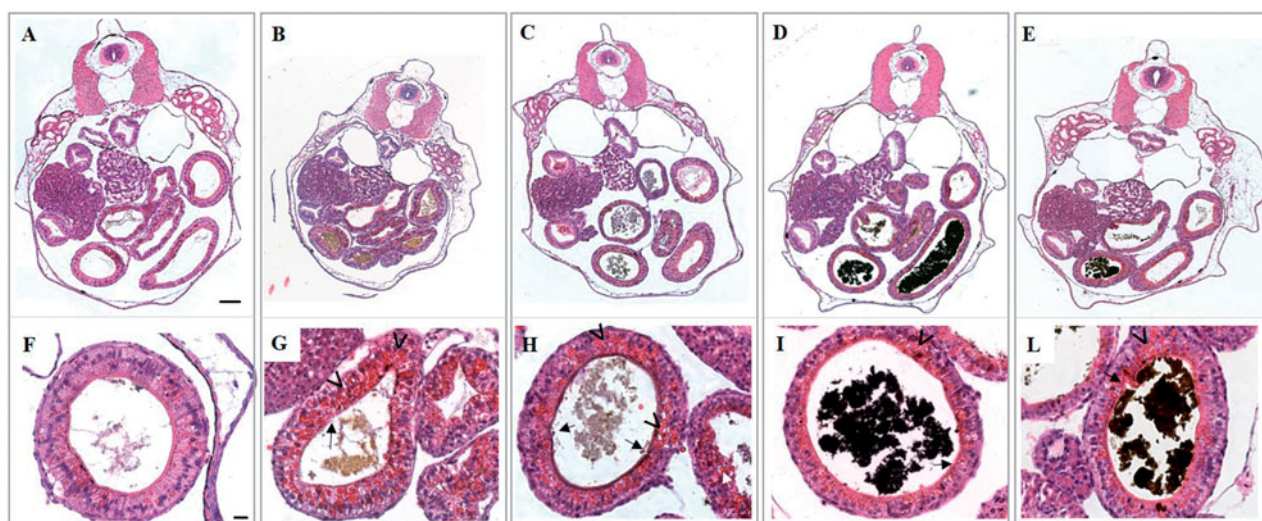


Figure 5. Histological transversal sections of stage 46 *X. laevis* embryos at level of abdominal region. Low (A–E) and high magnification (F–L) of a control (A and F) and embryos exposed to 25 mg Fe/L of FeSO_4 (B and G), FeCl_3 (C and H), ZVI NPs (D and I) and Fe_3O_4 NPs (E and L). In all treated embryos is appreciable the presence of material in the intestinal loops related to iron salts (B, C and G, H) and NPs (D, E and I, L). Damages at brush border (black arrow) and yolk platelets accumulation (arrowhead) in enterocytes are visible. Bars = 100 μm (low magnification) and 20 μm (high magnification).

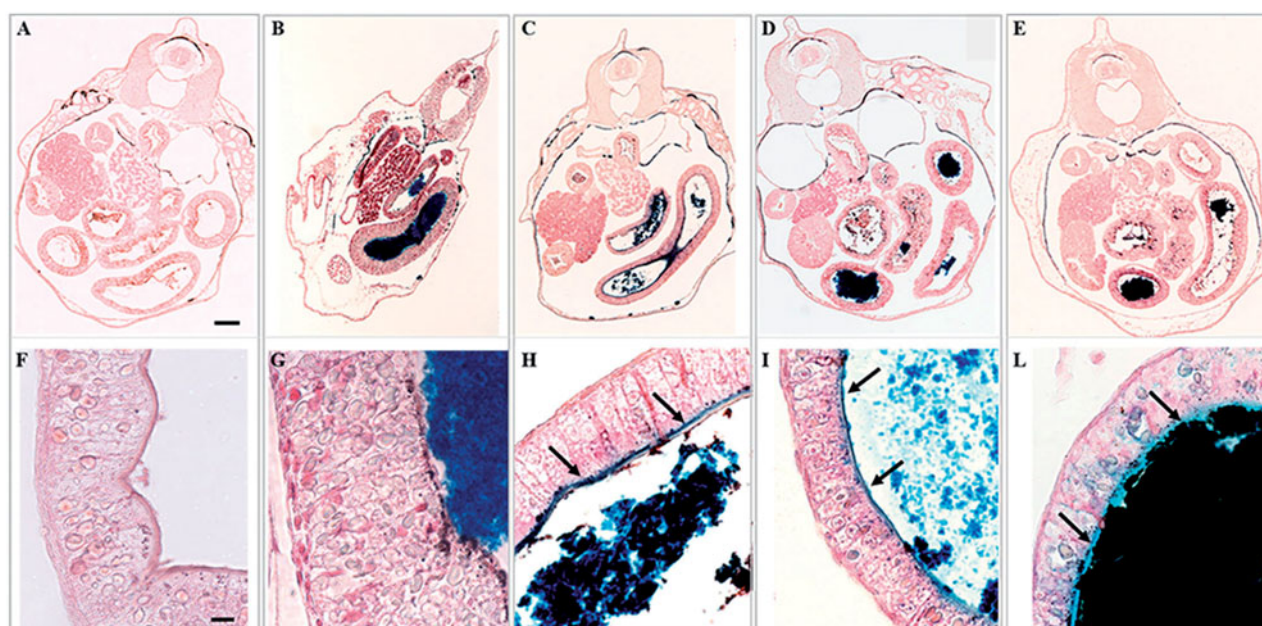


Figure 6. Histological transversal sections at abdominal region of stage 46 *X. laevis* embryos stained with Perl's protocol. Low (A–E) and high magnification (F–L) of a control (A and F) and embryos exposed to 25 mg Fe/L of FeSO_4 (B), FeCl_3 (C), ZVI NPs (D) and Fe_3O_4 NPs (E). In all treated embryos, the presence of blue material in the intestinal loops related to iron in form of Fe(III) is appreciable. In embryos treated with FeCl_3 (H), ZVI NPs (I) and Fe_3O_4 NPs (L), blue staining evidenced that iron adheres to the brush border (black arrow) Bars = 100 μm (low magnification) and 10 μm (high magnification).

obtained after treatments, being the iron content higher in the treated groups compared to the control group by a minimum of seven folds for FeCl_3 to a maximum of 150 folds for Fe_3O_4 NPs.

As expected, iron from FeSO_4 resulted more bioavailable than that from FeCl_3 , accumulating two fold more in embryonic tissues. Iron NPs treated

embryos, however, accumulated iron more efficiently than iron salt treated embryos; indeed, 8 (in ZVI NPs) to 11 (in Fe_3O_4 NPs) folds higher than in FeSO_4 treated embryos. Iron oxide NPs showed the highest bioconcentration factor (BCF) which resulted statistically different from both iron salts and from ZVI NPs (Figure 10).

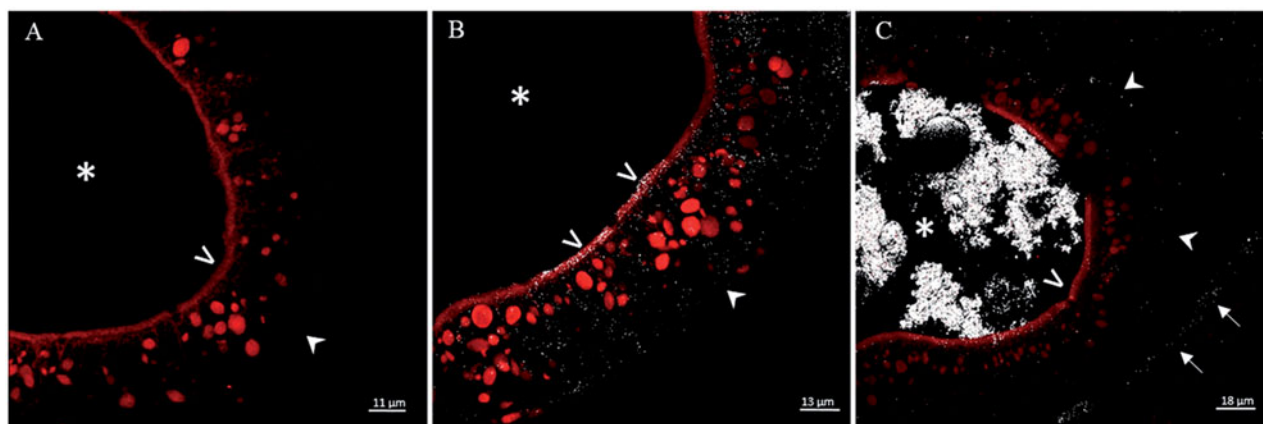


Figure 7. Laser scanning confocal microscopy in reflection mode on histological transversal sections at the level of small intestine of stage 46 *X. laevis* embryos. Control (A), and exposed to 25 mg Fe/L of ZVI NPs (B) and Fe_3O_4 NPs (C) embryos. Figure C is representative of an intestinal tract in which the nanoparticles have accumulated in the lumen. In treated embryos, NP reflection is visible in white color. (*) intestinal lumen; (>) brush border; (<) basement membrane; (←) serous membrane of the abdominal cavity.

Discussion

Different types of iron NPs are under scrutiny to be used in environmental and biomedical fields for several purposes. ZVI NPs have been mainly proposed in environmental remediation approaches for soil and water (Zhao et al. 2016; Li et al. 2017), while iron oxide NPs are extensively studied in nanomedicine for MRI and photothermal anticancer therapy (Kandasamy and Maity 2015; Ansari et al. 2018). Among the most promising applications of iron NPs, it has been recently suggested the use as diet supplementation or food fortification against iron deficiency (Blanco-Rojo and Vaquero 2019). This latter application may take advantage from the enhanced capability of iron NPs to be adsorbed by intestinal epithelial cells (Rohner et al. 2007; Acosta 2009; von Moos et al. 2017), overcoming the poor bioavailability of low soluble iron compounds and the remarkable side effects of those soluble in water and highly bioavailable.

Despite the huge amount of data in literature reporting attempts to improve iron NPs efficacy, relatively little is known on the toxic effects in relation to the modality of bio-nano interaction, in particular during development. In a review dedicated to the toxicity of iron oxide NPs, Valdiglesias and colleagues (Valdiglesias et al. 2015) pointed out the low number of studies dealing with the developmental toxicity and in general, the controversial results achieved for the cytotoxic, genotoxic and neurotoxic effects of iron NPs.

Among the vertebrate developmental models, zebrafish and *Xenopus* share similar experimental advantages regarding their usefulness in organism-based chemical screening during early development (Wheeler and Brandli 2009). Although zebrafish remains the most exploited, *Xenopus* as a tetrapod is evolutionarily closer to humans than zebrafish and allows impact assessment on organs more similar to their human counterparts than those found in zebrafish. In the contest of our study, the development of a convoluted intestine and the ability to swallow acquired within 96 h p.f. make the *Xenopus* embryos more feasible for evaluating the impact of particulate material through ingestion.

In previous papers, *Xenopus laevis* embryos have been effectively used as experimental model to screen the comparative toxicity of metal and metal oxide NPs (Bacchetta et al. 2012; Colombo et al. 2017). It has been demonstrated that different metal oxides, like CuO, ZnO and TiO_2 are able to exert variable embryotoxic effects (Bacchetta et al. 2012; Nations et al. 2011) and that the model is able to predict the teratogenicity of NMs, as in the case of surface coated Ag NPs (Colombo et al. 2017). Remarkably, the main target organ for the NMs studied always resulted to be the intestine. It occurs only at developmental stages following the stomodeum opening, when embryos begin to swallow NP suspensions (Bonfanti et al. 2015). At that point, ZnO NPs come in contact with the intestinal epithelium, where they are adsorbed through different mechanisms, induce oxidative damages and consequent

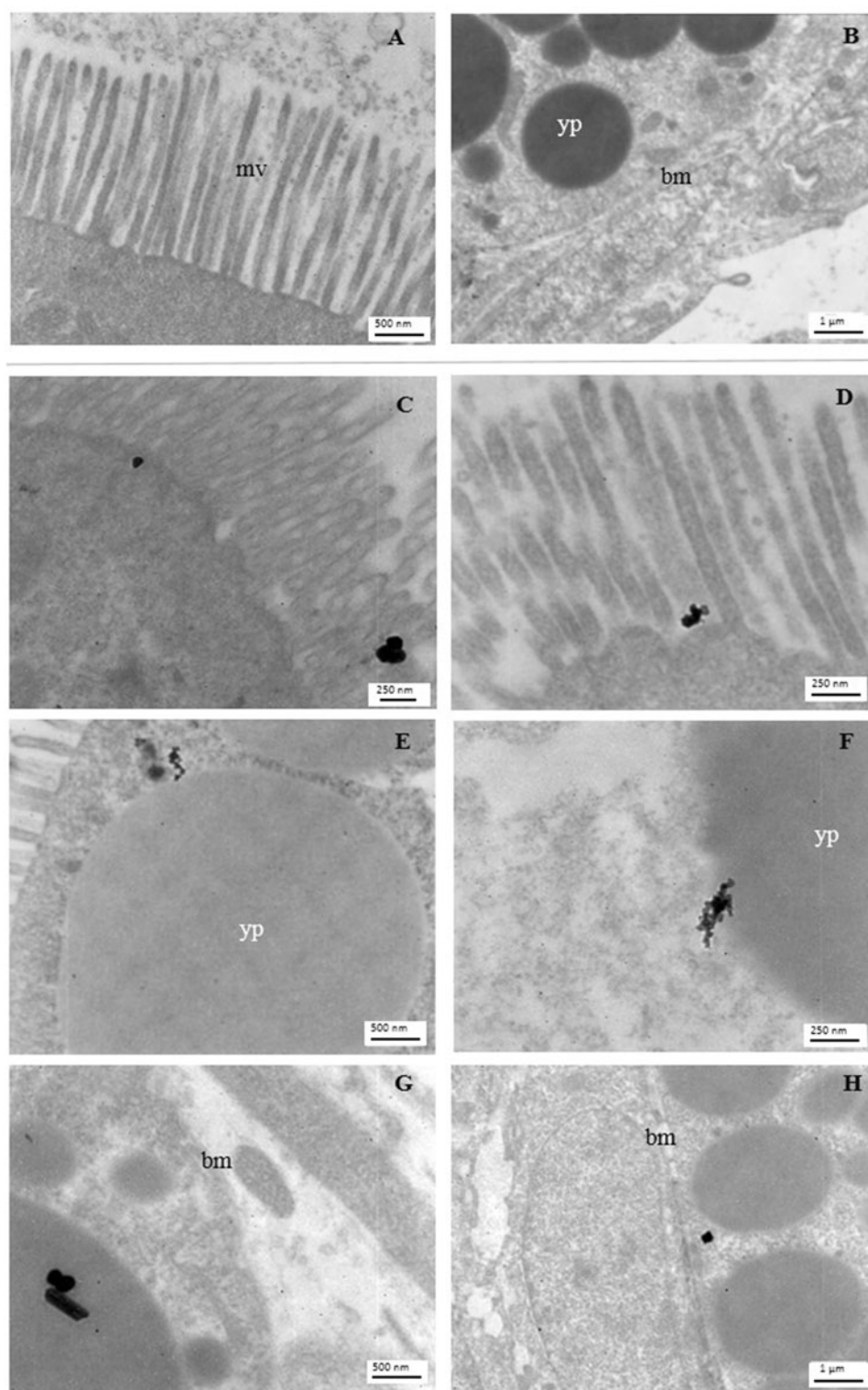


Figure 8. Electron microscopy imaging of the *X. laevis* small intestine. Apical and basal region of enterocytes of a control embryo (A and B, respectively) and embryos exposed to 25 mg Fe/L of ZVI NPs (C, E, G) or Fe_3O_4 NPs (D, F, H). NPs aggregates in treated embryos are clearly visible near to the microvilli (mv), yolk platelets (yp) and basement membrane (bm).

histological lesions to the intestinal mucosa (Bacchetta et al. 2014). Together, these evidences suggest that *Xenopus* embryos might be profitably adopted to study the absorption mechanism and

possible toxicity in a developing system of orally available NMs, like iron NPs that are potentially relevant for environmental or biomedical purposes. Moreover, it should be considered that *Xenopus*

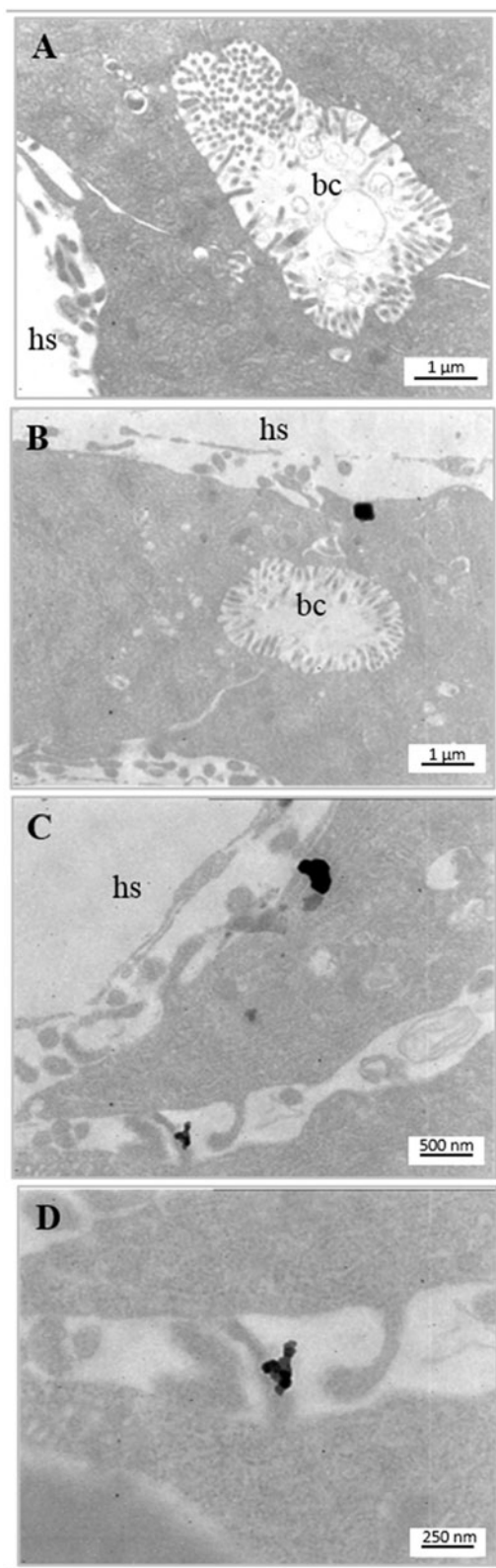


Figure 9. Electron microscopy imaging of the *X. laevis* liver. Bile canaliculus (bc) and hepatic sinusoid (hs) of control (A) and exposed to 25 mg Fe/L of Fe_3O_4 NPs (B–D) embryos. NPs aggregates in treated embryos are clearly visible in sinusoidal space and within hepatocytes (B, C). (D) High magnification of C.

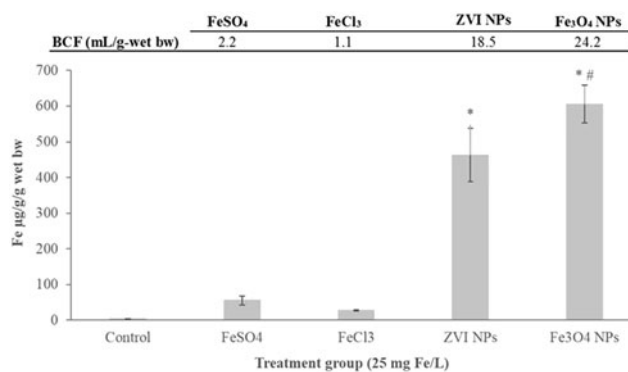


Figure 10. Total iron concentrations measured by ICP-OES in stage 46 embryos exposed during FETAX to Fe(II/III) salts and iron NPs at the nominal concentration of 25 mg Fe/L, with the correspondent bioconcentration factors (BCF). Data are mean \pm SE (n =three replicates per concentration; fifty embryos per replicate). (BCF, mL/g wet-bw)=iron concentration in embryos (mg/Kg wet-bw/nominal iron concentration in treatment solutions at 25 mg/L). (*) statistically different from control; (#) statistically different from the other iron treatments ($p < 0.05$, ANOVA + Fisher LSD Method).

embryos represent a valuable model to bridge *in vitro* and *in vivo* studies using mammals, with negligible ethical implications. To confirm this, a study by Webster and collaborators (Webster et al. 2016) showed that after exposure to a range of NPs, the phenotypic score of *Xenopus* embryos showed a strong correlation with *in vitro* cell tests and, in particular, magnetite cored NPs, negative for toxicity in *in vitro* and *Xenopus*, were further confirmed as non-toxic in mice.

Despite the extensive literature adopting human cells and mammals to investigate iron NP toxicity (Valdiglesias et al. 2015; von Moos et al. 2017), only few papers are based on alternative models. The effects of different Fe_2O_3 NPs were studied in *Xenopus* (Nations et al. 2011; Marin-Barba et al. 2018) and in zebrafish (Zhu, Tian, and Cai 2012), while the effects of ZVI and Fe_3O_4 NPs, in parallel to Fe bioaccumulation and oxidative stress were investigated in early life stages of medaka fish (Chen, Tan, and Wu 2012; Chen, Wu, and Wu 2013).

Considering the very few data available on iron NPs toxicity in developing vertebrate models and the promising application of *Xenopus* embryos in the study of the bio-nano interactions at the intestinal level, in the present work Fe_3O_4 and ZVI NPs effects have been tested by FETAX, followed by morphological studies on NP uptake and tissue

translocation. Exposure to iron NPs occurred in parallel to FeSO_4 and FeCl_3 to verify the toxicity of iron salts under comparable Fe nominal concentrations. We considered interesting the comparison between an oxide iron NP form, mainly applicable in biomedical and novel food and feed sectors, with the most reduced iron NP form, represented by the ZVI, which finds wide applications in soil and water remediation technologies, thanks to its high surface oxidative potential toward organic molecules (Chen, Wu, and Wu 2013). The two selected iron NPs showed similar size, shape and behavior in the FETAX solution with rapid agglomeration in micrometric clusters followed by precipitation, a condition that could frequently occur in the aquatic environment (Grieger et al. 2010). On the contrary, they differ in terms of surface charge, being the Fe_3O_4 NPs weakly cationic and the ZVI NPs weakly anionic. This difference is interesting because it is well known that electrostatic interaction of cationic NPs with negatively charged phospholipid head groups or protein domains on cell surfaces promotes local membrane deformation and NP internalization (Nel et al. 2006; Fleck and Netz 2004).

Our results demonstrate the almost negligible embryotoxicity of iron NPs in the concentration range 5-100 mg Fe/L, which is however higher than the relevant environmental concentrations estimated to be in the range 0-5 mg Fe/L (Chen, Tan, and Wu 2012). Both ZVI and Fe_3O_4 NPs did not induce lethality in embryos at any tested concentrations. Only the oxide caused a slight, but significant, increase in the malformed embryo percentages, with no concentration-dependent effect. The malformations mainly consisted in gut miscoiling, with abundant presence of particulate matter in the gut lumen; according to this result, also Marín-Barba and colleagues (Marin-Barba et al. 2018) described an intestinal inflammation as a consequence of the exposure of *Xenopus* embryos to high concentrations of Fe_2O_3 NPs. A more important effect of Fe_2O_3 NPs was instead shown in zebrafish embryos with hatching impairment at concentrations higher than 10 mg/L and a 168 h LC_{50} of 53.35 mg/L (Zhu, Tian, and Cai 2012). We believe that the observed increase in gut miscoiling by iron oxide NPs, albeit low, is to be related to their higher reactivity with cellular membranes due to their weak surface cationic charge evidenced by z potential. This

hypothesis is corroborated by our previous study in *Xenopus* embryos where, contrary to negatively charged Citrate-Ag NPs, cationic charged branched polyethylenimine-Ag NPs affected significantly embryo development inducing irregular intestinal diverticula (Colombo et al. 2017).

Considering embryonic growth, at all the ZVI and Fe_3O_4 NPs concentrations, our embryos showed a slight increase in body length. Undoubtedly, our iron NPs, having a very high PDI that makes them unstable in suspension, should be functionalized to be used in the food industry. However, this result is indicative of a beneficial effect deriving from the administration of an essential element in nanosized form, at least up to 100 mg Fe/L. Instead, in a FETAX study by Nations et al (2011), exposure of the embryos to a high concentration (1000 mg/L) of iron NPs different from ours (Fe_2O_3 NPs) resulted in a significant reduction in the total body length without recording acute toxicity effects.

Interestingly, contrary to iron NPs, in our study iron salts resulted severely embryotoxic. A concentration-dependent mortality has been characterized for both ferrous and ferric ions derived from FeSO_4 and FeCl_3 salts, respectively, with the latter being the strongest lethal agent as evidenced by 96 h p.f. LC_{50} (56.10 mg/L for FeSO_4 versus 32.21 mg/L for FeCl_3). Similar to the specimens exposed to iron NPs, gut resulted to be the most affected organ in iron salts treated embryos. Moreover, iron salts also affected embryo growth starting from concentration of 10 mg Fe/L, while at 5 mg/L an increase in the body length was observed, suggesting a possible hormetic effect.

Overall, based on FETAX results, it is clear that the iron NPs considered in this study are neither lethal nor teratogenic in *Xenopus* embryos, in contrast to iron salts. This differential impact on *Xenopus* development could be derived by the specific behavior in FETAX solution of the iron species tested. In particular, the acidification of the FETAX solution and the formation of aggregates of iron(III) oxo-hydroxides that have deposited on the fertilization envelope, probably inducing hypoxia, could be the causes of acute toxicity of iron salts.

A slightly higher acute mortality and sublethal developmental toxicity of Fe(II) in comparison to Fe_3O_4 NPs have been observed also by Chen and colleagues (Chen, Wu, and Wu 2013) in medaka

embryos even if at concentrations as high as 200 mg Fe/L. However, in the same paper the ZVI NPs stabilized in suspension with carboxymethyl cellulose were the most embryotoxic compared to Fe(II) and to the bare Fe₃O₄ NPs that settled quickly, probably due to their greater reactivity in the oxygenated solution, which caused hypoxia and production of reactive oxygen species (Chen, Wu, and Wu 2013).

Surprisingly, the 168 h LC₅₀ for Fe₂O₃ NPs found by Zhu et al. (Zhu, Tian, and Cai 2012) in zebrafish embryos is comparable to our FeSO₄ LC₅₀. The authors hypothesized that the release of metal ions from the iron oxide NPs is one of the causes to which this NP embryotoxicity in zebrafish can be attributed.

In light of the above, it can be argued that the low embryotoxicity of our iron NPs is mainly ascribable to the NP aggregation followed by a rapid sedimentation of aggregates in FETAX solution, which determines a reduction of the surface area with a consequent lower reactivity and negligible release of metal ions.

However, the uptake of NPs was not affected by sedimentation because the grazing behavior that characterizes *Xenopus* embryos after the stomodeum opening, led to a significant iron NPs ingestion as evidenced by histological analysis. Although not entirely absorbed by the epithelial barrier and/or distributed in the distal organs, iron NPs have been firmly retained inside the intestine with no obvious signs of damage to the intestinal epithelium and organs, such as the liver involved in the accumulation of iron. This finding supports previous studies in birds and mammals demonstrating the safety of oral ingested iron based nanomaterials (Rohner et al. 2007; Chamorro et al. 2015; von Moos et al. 2017). In particular, the development of higher intestinal villi, a morphological feature typical of birds fed with an iron-supplemented diet, was demonstrated in growing chickens administered orally with γ -Fe₂O₃ NPs (Chamorro et al. 2015). Similarly, iron NPs were detected by Pearl's staining in duodenum of rats fed with FePO₄ NPs supplemented diet without histological changes and excess of iron accumulation in organs (von Moos et al. 2017). Conversely, shorter and sparser intestinal villi with a thinner intestinal wall have been evidenced in medaka fish, but only in larvae exposed for a long period (7-days) at high concentration of ZVI NPs (100 mg/L) (Chen, Tan, and Wu 2012).

The persistence of iron NPs in the *Xenopus* embryo intestinal tract may have prolonged their availability for absorption by increasing their bioaccumulation factor to a greater extent than FeSO₄, known as the reference salt in studies on bioavailability (Blanco-Rojo and Vaquero 2019). Similar BCF values were obtained for Fe₃O₄ NPs in medaka fish embryos, which showed an easier accumulation of iron NPs compared to Fe(II) due to the increasing exposure of embryos residing on the container bottom to the sedimented particles (Chen, Wu, and Wu 2013). However, in our study, despite a purging of 36 h, the possible small NP residues in the intestinal lumen, verified by Prussian blue staining in the histological sections (data not shown), may have contributed to the large difference in iron content between embryos treated with NPs and salts.

It is noteworthy that the most evident Fe signal revealed by histochemistry was found in embryos exposed to iron NPs, with evident blue staining not only at the brush border level, but also distributed in the cytoplasm of the enterocytes. Considering together NP tracking analyses by confocal and electron microscopy, supported by the bioconcentration factors, it appears that iron NPs are efficiently taken up by intestinal epithelium and in the case of iron oxide transferred also to hepatocytes. This is consistent with the hypothesis above mentioned of a higher reactivity of the positive surface charged Fe₃O₄ NPs that makes them more prone to interact electrostatically with the negatively charged surface of the outer cell membrane, to be internalized and translocated to non-target organs.

While the different pathways involved in the absorption of various iron species in duodenal enterocytes are well-documented (Blanco-Rojo and Vaquero 2019), the mechanisms by which iron NPs are internalized are less consolidated since the pathway is conditioned by the physico-chemical properties of NPs such as size and charge. Considering the size, endocytosis is the canonical pathway feasible for iron NPs (Perfecto et al. 2017), while when the permeability of the tight junctions between enterocytes is increased, NPs less than 50 nm in diameter pass through the paracellular route (Jahn et al. 2012). However, based on transport and TEM studies in Caco-2 cells, a mechanism of diffusion across enterocyte plasma membrane has been hypothesized for FeO NPs with a neutral hydrophilic shell (Jahn et al. 2012). By means of

electrophysiological studies, Zanella and colleagues (Zanella et al. 2017) demonstrated that, unlike ZVI NPs, positive poorly charged and naked Fe_3O_4 NPs, the same we studied here, penetrate through the lipid bilayer of a model system such as *Xenopus laevis* oocytes by simple diffusion. The authors explained this different behavior speculating a slower rate of aggregation of Fe_3O_4 NPs in comparison to ZVI NPs, which makes available for the interaction with plasma membrane an iron oxide sub-micron population.

Differently from *Xenopus* oocytes, in our experimental model the more complex intestinal environment (i.e. changes in pH, presence of bacteria, mucins and other secretions) makes the understanding of the mechanisms that regulate the passage through the intestinal barrier more complicated. Although our iron NPs form large aggregates, from TEM images the NPs in the cytoplasm of enterocytes do not appear to be included in vesicles excluding the endocytic pathway. Therefore, we hypothesize that small clusters of NPs may originate in the intestinal lumen and diffuse through enterocytes plasma membrane. Moreover, also a paracellular route is suggested by the confocal tracking analysis. However, the mechanisms of iron NP transport, that are here only speculated, need to be elucidated with further studies.

Conclusion

In this study, we propose *Xenopus laevis* embryos as a model to assess the impact and bio-interaction of Fe_3O_4 and ZVI NPs with respect to Fe(II) and (III) salts by combining the FETAX approach with the morphological evaluation of the effects on the intestinal barrier. Indeed, during the first 96 h p.f. *Xenopus* embryos develop a primitive – but morphologically differentiated - intestine and a grazing behavior leading to material ingestion. These peculiarities place them as a model of simple whole organism, ethically more acceptable than mammals and more complex than *in vitro* systems of mono- or co-cultures, for the primary screening of the NP potential in inducing tissue damage or being internalized by intestinal cells.

We have demonstrated that, unlike ferrous and ferric ions, Fe_3O_4 and ZVI NPs are neither embryotoxic nor teratogenic and have a slight positive effect on the embryo growth likely derived from a higher intake of an essential element. Furthermore, iron NPs accumulate abundantly after ingestion in

the intestinal lumen without causing morphological damage to intestinal epithelium and to other embryo organs such as liver. Iron NPs were mapped into enterocytes, along the paracellular spaces, at the level of the basement membrane of the intestinal epithelium and in the case of iron oxide NPs also in the liver. The presence of NPs apparently not included in vesicles in the cytoplasm of enterocytes suggests that they can be internalized not by canonical endocytic pathway but by diffusion of small NP clusters across the plasma membrane.

Taken together, these results improve our knowledge on the safety of the orally ingested iron NPs, and on their interaction with the intestinal barrier so far limited mainly to mammals and cell cultures. Taking into account the limits of the use of unstable NPs, these data could be useful as a first step in defining the potential risks associated with the various applications of iron NPs, whether they are applied in environmental remediation or in food/feed fortification. Since the surface coating is an important factor affecting the biological interactions of NPs, further investigations on iron NPs with different coatings and characteristics are highly desirable.

Acknowledgments

The authors wish to thank Prof. Maddalena Collini, Department of Physics, University of Milano-Bicocca for the confocal microscopy facility, Dr. Umberto Fascio for his precious support in confocal laser scanning microscopy analyses, and Dr. Tiziano Catelani for TEM NP images.

Disclosure statement

No potential conflict of interest was reported by the authors.

Funding

This work was supported by the University of Milano-Bicocca [grant number 2018-ATE-0424 to AC] and by the HOTZYMES project (grant agreement n° 829162) under EU's Horizon 2020 Programme (H2020-FETOPEN-2018-2019-2020-01) to GB. FG is recipient of a fellowship granted from 'Associazione Amici dell'Università dell'Insubria'.

References

- Acosta, E. 2009. "Bioavailability of Nanoparticles in Nutrient and Nutraceutical Delivery." *Current Opinion in Colloid & Interface Science* 14(1): 3–15. doi:10.1016/j.cocis.2008.01.002.

- Ansari, M. O., M. F. Ahmad, G. G. H. A. Shadab, and H. R. Siddique. 2018. "Superparamagnetic Iron Oxide Nanoparticles Based Cancer Theranostics: A Double Edge Sword to Fight against Cancer." *Journal of Drug Delivery Science and Technology* 45: 177–183. doi:10.1016/j.jddst.2018.03.017.
- Armenia, Ilaria, María Valeria Grazú Bonavia, Laura De Matteis, Pavlo Ivanchenko, Gianmario Martra, Rosalba Gornati, Jesus M. de la Fuente, and Giovanni Bernardini. 2019. "Enzyme Activation by Alternating Magnetic Field: Importance of the Bioconjugation Methodology." *Journal of Colloid and Interface Science* 537: 615–628. doi:10.1016/j.jcis.2018.11.058.
- Armenia, Ilaria, Giorgia Letizia Marcone, Francesca Berini, Viviana Teresa Orlandi, Cristina Pirrone, Eleonora Martegani, Rosalba Gornati, Giovanni Bernardini, and Flavia Marinelli. 2018. "Magnetic Nanoconjugated Teicoplanin: A Novel Tool for Bacterial Infection Site Targeting." *Frontiers in Microbiology* 9: 2270. doi:10.3389/fmicb.2018.02270.
- Bacchetta, R., E. Moschini, N. Santo, U. Fascio, L. Del Giacco, S. Freddi, M. Camatini, P. Mantecca. 2014. "Evidence and Uptake Routes for Zinc Oxide Nanoparticles through the Gastrointestinal Barrier in *Xenopus laevis*." *Nanotoxicology* 8(7): 728–744. doi:10.3109/17435390.2013.824128.
- Bacchetta, Renato, Nadia Santo, Umberto Fascio, Elisa Moschini, Stefano Freddi, Giuseppe Chirico, Marina Camatini, and Paride Mantecca. 2012. "Nano-Sized CuO, TiO₂ and ZnO Affect *Xenopus laevis* Development." *Nanotoxicology* 6(4): 381–398. doi:10.3109/17435390.2011.579634.
- Balzaretti, Riccardo, Fabian Meder, Marco P. Monopoli, Luca Boselli, Ilaria Armenia, Loredano Pollegioni, Giovanni Bernardini, and Rosalba Gornati. 2017. "Synthesis, Characterization and Programmable Toxicity of Iron Oxide Nanoparticles Conjugated with D-Amino Acid Oxidase." *Rsc Advances* 7(3): 1439–1442. doi:10.1039/C6RA25349K.
- Bernardini, G., C. Vismara, P. Boracchi, and M. Camatini. 1994. "Lethality, Teratogenicity and Growth Inhibition of Heptanol in *Xenopus* Assayed by a Modified Frog Embryo Teratogenesis assay-*Xenopus* (FETAX) Procedure." *Science of the Total Environment* 151(1): 1–8. doi:10.1016/0048-9697(94)90480-4.
- Blanco-Rojo, R., and M. P. Vaquero. 2019. "Iron Bioavailability from Food Fortification to Precision Nutrition. A Review." *Innovative Food Science & Emerging Technologies* 51: 126–138. doi:10.1016/j.ifset.2018.04.015.
- Bonfanti, Patrizia, Elisa Moschini, Melissa Saibene, Renato Bacchetta, Leonardo Rettighieri, Lorenzo Calabri, Anita Colombo, and Paride Mantecca. 2015. "Do Nanoparticle Physico-Chemical Properties and Developmental Exposure Window Influence Nano ZnO Embryotoxicity in *Xenopus laevis*?" *International Journal of Environmental Research and Public Health* 12(8): 8828–8848.
- Bonfanti, P., M. Saibene, R. Bacchetta, P. Mantecca, and A. Colombo. 2018. "A Glyphosate Micro-Emulsion Formulation Displays Teratogenicity in *Xenopus laevis*." *Aquatic Toxicology (Toxicology)* 195: 103–113. doi:10.1016/j.aquatox.2017.12.007.
- Camaschella, C. 2019. "Iron Deficiency." *Blood* 133(1): 30–39. doi:10.1182/blood-2018-05-815944.
- Cappellini, Francesca, Camilla Recordati, Marcella De Maglie, Loredano Pollegioni, Federica Rossi, Marco Daturi, Rosalba Gornati, and Giovanni Bernardini. 2015. "New Synthesis and Biodistribution of the D-Amino Acid Oxidase-Magnetic Nanoparticle System." *Future Science OA* 1(4): FSO67.
- Chamorro, Susana, Lucía Gutiérrez, María Pilar Vaquero, Dolores Verdoy, Gorka Salas, Yurena Luengo, Agustín Brenes, and Francisco José Teran. 2015. "Safety Assessment of Chronic Oral Exposure to Iron Oxide Nanoparticles." *Nanotechnology* 26(20): 205101. doi:10.1088/0957-4484/26/20/205101.
- Chen, P.-J., S.-W. Tan, and W.-L. Wu. 2012. "Stabilization or Oxidation of Nanoscale Zerovalent Iron at Environmentally Relevant Exposure Changes Bioavailability and Toxicity in Medaka Fish." *Environmental Science Technology*. 46(15): 8431–8439.
- Chen, P.-J., W.-L. Wu, and K. C.-W. Wu. 2013. "The Zerovalent Iron Nanoparticle Causes Higher Developmental Toxicity than Its Oxidation Products in Early Life Stages of Medaka Fish." *Water Research* 47(12): 3899–3909.
- Chenon, P., L. Gauthier, P. Loubieres, A. Severac, and M. Delpoux. 2003. "Evaluation of the Genotoxic and Teratogenic Potential of a Municipal Sludge and Sludge-Amended Soil Using the Amphibian *Xenopus laevis* and the Tobacco: *Nicotiana tabacum* L. var. xanthi Dulieu." *Science of the Total Environment* 301(1–3): 139–150. doi:10.1016/S0048-9697(02)00287-5.
- Coccini, T., U. De Simone, M. Roccio, S. Croce, E. Lenta, M. Zecca, A. Spinillo, and M. A. Avanzini. 2019. "In Vitro Toxicity Screening of Magnetite Nanoparticles by Applying Mesenchymal Stem Cells Derived from Human Umbilical Cord Lining." *Journal of Applied Toxicology* 39(9): 1320–1336. doi:10.1002/jat.3819.
- Colombo, Anita, Melissa Saibene, Elisa Moschini, Patrizia Bonfanti, Maddalena Collini, Kaja Kasemets, and Paride Mantecca. 2017. "Teratogenic Hazard of BPEI-Coated Silver Nanoparticles to *Xenopus laevis*." *Nanotoxicology* 11(3): 405–418. doi:10.1080/17435390.2017.1309703.
- Dawson, D. A. 1991. "Additive Incidence of Developmental Malformation for *Xenopus* Embryos Exposed to a Mixture of Ten Aliphatic Carboxylic Acids." *Teratology* 44(5): 531–546.
- Dumont, J., N. T. W. Schultz, M. V. Buchanan, and G. L. Kao. 1983. "Frog Embryo Teratogenesis Assay: *Xenopus* (FETAX) – a Short-Term Assay Applicable to Complex Environmental Mixtures." In *Short-Term Bioassays in the Analysis of Complex Environmental Mixtures III Environmental Science Research Vol 27*, edited by Waters M.D., Lewtas J., Claxton L., Chernoff N., Nesnow S, 393–405. Boston, MA: Springer.
- Feng, Q., Y. Liu, J. Huang, K. Chen, J. Huang, and K. Xiao. 2018. "Uptake, Distribution, Clearance, and Toxicity of Iron

- Oxide Nanoparticles with Different Sizes and Coatings." *Scientific Reports* 8(1): 2082. doi:10.1038/s41598-018-19628-z.
- Fleck, C. C., and R. R. Netz. 2004. "Electrostatic Colloid-Membrane Binding." *Europhysics Letters (Epl)* 67(2): 314–320. doi:10.1209/epl/i2004-10068-x.
- Fort, D., D. McLaughlin, and J. Burkhart. 2003. "The FETAX of Today — and Tomorrow." In *STP1443-EB Multiple Stressor Effects in Relation to Declining Amphibian Populations*, edited by Linder, Krest S, Sparling D, Little E, 23–45. West Conshohocken, PA: ASTM International. doi:10.1520/STP111735.
- Fort, D. J., D. W. McLaughlin, R. L. Rogers, and B. O. Buzzard. 2003. "Evaluation of the Developmental Toxicities of Ethanol, Acetaldehyde, and Thioacetamide Using FETAX." *Drug and Chemical Toxicology* 26(1): 23–34. doi:10.1081/DCT-120017555.
- Fort, D. J., and R. Robbin. 2002. "Enhancing the Predictive Validity of Frog Embryo Teratogenesis Assay—Xenopus (FETAX)." *Journal of Applied Toxicology* 22(3): 185–191. doi:10.1002/jat.848.
- Garber, E. A. E., J. L. Erb, J. Magner, and G. Larsen. 2004. "Low Levels of Sodium and Potassium in the Water from Wetlands in Minnesota That Contained Malformed Frogs Affect the Rate of Xenopus Development." *Environmental Monitoring and Assessment* 90(1–3): 45–64. doi:10.1023/B:EMAS.0000003565.25474.8f.
- Gornati, Rosalba, Elisa Pedretti, Federica Rossi, Francesca Cappellini, Michela Zanella, Iolanda Olivato, Enrico Sabbioni, and Giovanni Bernardini. 2016. "Zerovalent Fe, Co and Ni Nanoparticle Toxicity Evaluated on SKOV-3 and U87 Cell Lines." *Journal of Applied Toxicology* 36(3): 385–393. doi:10.1002/jat.3220.
- Grieger, K. D., A. Fjordbøge, N. B. Hartmann, E. Eriksson, P. L. Bjerg, and A. Baun. 2010. "Environmental Benefits and Risks of Zero-Valent Iron Nanoparticles (nZVI) for in Situ Remediation: Risk Mitigation or Trade-off?" *Journal of Contaminant Hydrology* 118(3-4): 165–183. doi:10.1016/j.jconhyd.2010.07.011.
- Hausen, P., and M. Riebesell. 1991. *The Early Development of Xenopus Laevis: An Atlas of the Histology*. Berlin and Heidelberg: Springer-Verlag.
- Hilty, Florentine M., Myrtha Arnold, Monika Hilbe, Alexandra Teleki, Jesper T. N. Knijnenburg, Felix Ehrensperger, Richard F. Hurrell, Sotiris E. Pratsinis, Wolfgang Langhans, Michael B. Zimmermann, et al. 2010. "Iron from Nanocompounds Containing Iron and Zinc Is Highly Bioavailable in Rats without Tissue Accumulation." *Nature Nanotechnology* 5(5): 374–380. doi:10.1038/nnano.2010.79.
- Hosny, K. M., Z. M. Banjar, A. H. Hariri, and A. H. Hassan. 2015. "Solid Lipid Nanoparticles Loaded with Iron to Overcome Barriers for Treatment of Iron Deficiency anemia." *Drug Design, Development and Therapy* 9: 313–320. doi:10.2147/DDDT.S77702.
- Jahn, M. R., T. Nawroth, S. Futterer, U. Wolfrum, U. Kolb, and P. Langguth. 2012. "Iron Oxide/Hydroxide Nanoparticles with Negatively Charged Shells Show Increased Uptake in Caco-2 Cells." *Molecular Pharmaceutics* 9(6): 1628–1637.
- Kandasamy, G., and D. Maity. 2015. "Recent Advances in Superparamagnetic Iron Oxide Nanoparticles (SPIONs) for in Vitro and in Vivo Cancer Nanotheranostics." *International Journal of Pharmaceutics* 496(2): 191–218. doi:10.1016/j.ijpharm.2015.10.058.
- Kassebaum, N. J., G. B. D. A. Collaborators, T. D. Fleming. 2016. "The Global Burden of Anemia." *Hematology/Oncology Clinics of North America* 30(2): 247–308. doi:10.1016/j.hoc.2015.11.002.
- Li, S., W. Wang, F. Liang, and W.-X. Zhang. 2017. "Heavy Metal Removal Using Nanoscale Zero-Valent Iron (nZVI): Theory and Application." *Journal of Hazardous Materials* 322(Pt A): 163–171. doi:10.1016/j.jhazmat.2016.01.032.
- Marin-Barba, M., H. Gavilan, L. Gutierrez, Lozano-Velasco E, Rodríguez-Ramiro I, Wheeler G. N., Morris C. J., Morales M. P., Ruiz A. 2018. "Unravelling the Mechanisms That Determine the Uptake and Metabolism of Magnetic Single and Multicore Nanoparticles in a *Xenopus laevis* Model." *Nanoscale* 10(2): 690–704.
- Moros, M., J. Idiago-Lopez, L. Asin, E. Moreno-Antolín, L. Beola, V. Grazú, R. M. Fratila, L. Gutiérrez, J. M. de la Fuente. 2018. "Triggering Antitumoural Drug Release and Gene Expression by Magnetic Hyperthermia." *Advanced Drug Delivery Reviews* 138: 326–343.
- Nations, S., M. Wages, J. E. Canas, J. Maul, C. Theodorakis, and G. P. Cobb. 2011. "Acute Effects of Fe2O3, TiO2, ZnO and CuO Nanomaterials on *Xenopus laevis*." *Chemosphere* 83(8): 1053–1061. doi:10.1016/j.chemosphere.2011.01.061.
- Nel, A., T. Xia, L. Mädler, and N. Li. 2006. "Toxic Potential of Materials at the Nanolevel." *Science* 311(5761): 622–627. doi:10.1126/science.1114397.
- Nieuwkoop, P., and J. Faber. 1956. *Normal Table of Xenopus laevis (Daudin): A Systematical and Chronologica Survey of the Development from the Fertilized Egg till the End of Metamorphosis* Amsterdam: North Holland Publishing Co.
- Perfecto, A., C. Elgy, E. Valsami-Jones, P. Sharp, F. Hilty, and S. Fairweather-Tait. 2017. "Mechanisms of Iron Uptake from Ferric Phosphate Nanoparticles in Human Intestinal Caco-2 Cells." *Nutrients* 9(4): 359. doi:10.3390/nu9040359.
- Prati, M., E. Biganzoli, P. Boracchi, M. Tesauro, C. Monetti, and G. Bernardini. 2000. "Ecotoxicological Soil Evaluation by FETAX." *Chemosphere* 41(10): 1621–1628. doi:10.1016/S0045-6535(00)00034-5.
- Prati, Mariangela, Rosalba Gornati, Patrizia Boracchi, Elia Biganzoli, Salvador Fortaner, Romano Pietra, Enrico Sabbioni, and Giovanni Bernardini. 2002. "A Comparative Study of the Toxicity of Mercury Dichloride and Methylmercury, Assayed by the Frog Embryo Teratogenesis Assay—Xenopus (FETAX)." *Alternatives to Laboratory Animals* 30(1): 23–32. doi:10.1177/026119290203000104.
- Presutti, C., C. Vismara, M. Camatini, and G. Bernardini. 1994. "Ecotoxicological Effects of a Nonionic Detergent (Triton DF-16) Assayed by modFETAX." *Bulletin of Environmental Contamination and Toxicology* 53(3): 405–411.

- Prins, F. A., I. C. Velde, and E. de Heer. 2006. "Reflection Contrast Microscopy: The Bridge between Light and Electron Microscopy." *Methods in Molecular Biology* 319: 363–401.
- Rohner, Fabian, Frank O. Ernst, Myrtha Arnold, Monika Hilbe, Ralf Biebinger, Frank Ehrensperger, Sotiris E. Pratsinis, Wolfgang Langhans, Richard F. Hurrell, Michael B. Zimmermann., et al. 2007. "Synthesis, Characterization, and Bioavailability in Rats of Ferric Phosphate Nanoparticles." *The Journal of Nutrition* 137(3): 614–619.
- Song, C., W. Sun, Y. Xiao, and X. Shi. 2019. "Ultrasmall Iron Oxide Nanoparticles: Synthesis, Surface Modification, Assembly, and Biomedical Applications." *Drug Discovery Today*.
- Tolkien, Z., L. Stecher, A. P. Mander, D. I. Pereira, and J. J. Powell. 2015. "Ferrous Sulfate Supplementation Causes Significant Gastrointestinal Side-Effects in Adults: A Systematic Review and Meta-Analysis." *PLoS One* 10(2): e0117383. doi:10.1371/journal.pone.0117383.
- Valdiglesias, Vanessa, Gözde Kiliç, Carla Costa, Natalia Fernández-Bertólez, Eduardo Pásaro, João Paulo Teixeira, and Blanca Laffon. 2015. "Effects of Iron Oxide Nanoparticles: Cytotoxicity, Genotoxicity, Developmental Toxicity, and Neurotoxicity." *Environmental and Molecular Mutagenesis* 56(2): 125–148.
- Vismara, C., G. Bernardini, P. Bonfanti, A. Colombo, and M. Camatini. 1993. "The Use of in Vitro Fertilization in the Frog Embryo Teratogenesis Assay in *Xenopus* (FETAX) and Its Applications to Ecotoxicology." *The Science of the Total Environment* 134 Suppl Pt 1: 787–790.
- von Moos, Lea M., Mirjam Schneider, Florentine M. Hilty, Monika Hilbe, Myrtha Arnold, Nathalie Ziegler, Diogo Sales Mato, Hans Winkler, Mohamed Tarik, Christian Ludwig., et al. 2017. "Iron Phosphate Nanoparticles for Food Fortification: Biological Effects in Rats and Human Cell Lines." *Nanotoxicology* 11(4): 496–506. doi:10.1080/17435390.2017.1314035.
- Webster, C. A., D. Di Silvio, A. Devarajan, P. Bigini, E. Micotti, C. Giudice, M. Salmona, G. N. Wheeler, V. Sherwood, and F. B. Bombelli. 2016. "An Early Developmental Vertebrate Model for Nanomaterial Safety: Bridging Cell-Based and Mammalian Toxicity Assessment." *Nanomedicine* 11(6): 643–656. doi:10.2217/nnm.15.219.
- Wheeler, G. N., and A. W. Brandli. 2009. "Simple Vertebrate Models for Chemical Genetics and Drug Discovery Screens: Lessons from Zebrafish and *Xenopus*." *Developmental Dynamics* 238(6): 1287–1308. doi:10.1002/dvdy.21967.
- Yu, M. R., Y. W. Yang, C. L. Zhu, S. Y. Guo, and Y. Gan. 2016. "Advances in the Transepithelial Transport of Nanoparticles." *Drug Discovery Today* 21(7): 1155–1161. doi:10.1016/j.drudis.2016.05.007.
- Zanella, D., E. Bossi, R. Gornati, C. Bastos, N. Faria, and G. Bernardini. 2017. "Iron Oxide Nanoparticles Can Cross Plasma Membranes." *Scientific Reports* 7. doi:10.1038/s41598-017-11535-z.
- Zhao, X., W. Liu, Z. Cai, B. Han, T. Qian, and D. Zhao. 2016. "An Overview of Preparation and Applications of Stabilized Zero-Valent Iron Nanoparticles for Soil and Groundwater Remediation." *Water Research* 100: 245–266. doi:10.1016/j.watres.2016.05.019.
- Zhu, X., S. Tian, and Z. Cai. 2012. "Toxicity Assessment of Iron Oxide Nanoparticles in Zebrafish (*Danio rerio*) Early Life Stages." *PLoS One* 7(9): e46286. doi:10.1371/journal.pone.0046286.
- Zimmermann, M. B., R. Biebinger, I. Egli, C. Zeder, and R. F. Hurrell. 2011. "Iron Deficiency up-Regulates Iron Absorption from Ferrous Sulphate but Not Ferric Pyrophosphate and Consequently Food Fortification with Ferrous Sulphate Has Relatively Greater Efficacy in Iron-Deficient Individuals." *British Journal of Nutrition* 105(8): 1245–1250. doi:10.1017/S0007114510004903.